Organic cages

DOI: 10.1002/anie.201105104

# Large Self-Assembled Chiral Organic Cages: Synthesis, Structure, and Shape Persistence**

*Kim E. Jelfs, Xiaofeng Wu, Marc Schmidtmann, James T. A. Jones, John E. Warren, Dave J. Adams, and Andrew I. Cooper**

Molecular organic cages—defined herein as shape-persistent organic molecules with permanent, accessible cavities[1]—have attracted wide interest because of their importance as host–guest systems,[2,3] as porous materials,[4–10] as catenanes,[11] and for nanoconfined chemical reactions.[12] Cage synthesis through imine condensation between aldehydes and amines has been shown to be effective and atom-economical.[1,6,13–16] Dynamic imine reactions[17] allow one-pot cage syntheses in yields that are often much higher than those obtained by irreversible routes.[17] It is still challenging, however, to synthesize discrete covalent organic cages of a size that can accommodate large guests, or multiple guests. Also, mesoporous molecular analogues of covalent organic framework materials[18] would require larger shape-persistent cages.

Building on earlier work by Cram et al.[19] and others, Warmuth and coworkers pioneered the construction of large organic imine cages.[20–23] This elegant work has led to nanocontainers,[20,21] rhombicuboctahedral nanocapsules,[22] and a chiral nanocube[23] using structurally defined, "pro-hollow" cavitands as building blocks. These organic molecules can reach impressive sizes: for example, the [6+8] giant rhombicuboctahedron[22] was estimated to have a solvodynamic diameter of 3.9 nm, and molecular models suggested a cavity volume of around 4700 Å$^3$. Unfortunately, crystals suitable for X-ray diffraction could not be obtained and structures were therefore inferred from a combination of NMR spectroscopy and molecular mechanics calculations.[20–23]

Herein, we describe the synthesis and structure of two large self-assembled covalent cage molecules, **CC7** and **CC8**. To our knowledge, these are the largest covalent organic cages to be characterized by single-crystal X-ray structure determination, although X-ray structures for even larger metal coordination cages have been reported.[24] The cages were obtained through [8+12] imine condensation reactions between two relatively simple precursors, tris(4-formylphenyl)amine (Scheme 1, **A**) and the chiral diamines (*R*,*R*)-1,2-cyclohexanediamine (**B1**) and (*R*,*R*)-1,2-cyclohex-4-enediamine (**B2**) to yield **CC7** and **CC8**, respectively. The reaction occurs without any additional template or catalyst (Scheme 1) to generate the $\mathbf{A}_8\mathbf{B}_{12}$ cage in good yield (85–90 %) through formation of 24 new imine bonds.

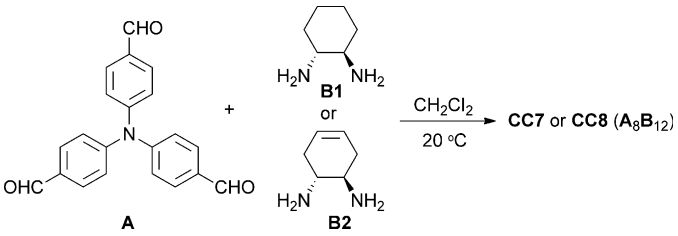


***Scheme 1.*** One-pot [8+12] synthesis of cages **CC7** and **CC8**.

Structural characterization of **CC7** and **CC8** by single-crystal X-ray diffraction proved challenging due to rapid solvent loss and associated decomposition of the single crystals when removed from the reaction solution.[20–23] In air, the crystals become opaque and crack within seconds; this also occurs in perfluoropolyether oil and other oils typically used in crystallography as protective media. Eventually, mesitylene was found to be a protective medium in which crystals of **CC7** and **CC8** are stable for minutes rather than seconds. The results of the structure elucidation are shown in Figure 1.

**CC7** crystallizes in the cubic space group $P2_13$ ($a$ = 47.266 Å, $V$ = 105 593 Å$^3$) with two crystallographically independent molecules, each located on a 3-fold axis (Figure S3). **CC8** crystallizes isostructurally, with slightly reduced unit cell parameters ($a$ = 46.875 Å, $V$ = 102 999 Å$^3$). The cage molecules **CC7** and **CC8** are packed only loosely into the three-dimensional structure (Figure 2), giving rise to large internal and external voids which are filled with the solvent dichloromethane.

In fact, disordered dichloromethane is the major constituent of the crystalline phase and it occupies more than 70 % of the available solvent-accessible volume—in total, about 75 000 Å$^3$ per unit cell. This amounts to around 80 and 75 dichloromethane molecules per cage molecule for **CC7** and **CC8**, respectively, although we cannot exclude the possibility that some of the protective medium, mesitylene, also diffuses

[*] Dr. K. E. Jelfs,[+] Dr. X. F. Wu,[+] Dr. M. Schmidtmann, Dr. J. T. A. Jones, Dr. J. E. Warren, Dr. D. J. Adams, Prof. A. I. Cooper
Department of Chemistry, Centre for Materials Discovery
University of Liverpool
Crown Street, Liverpool, L69 7ZD (UK)
E-mail: aicooper@liv.ac.uk

[+] These authors contributed equally.

[**] We thank the Engineering and Research Council (EPSRC; EP/H000925/1) and the Dutch Polymer Institute for financial support. A.I.C. is a Royal Society Wolfson Research Merit Award holder. We thank the STFC for access to Diamond Light Source and the staff at beamline I19. This work made use of the facilities of HECToR through our membership of the UK's HPC Materials Chemistry Consortium (EPSRC EP/F067496). We thank D. Willock and D. Holden for the molecular force fields, and G. Tribello for helpful discussions.

Supporting information for this article is available on the WWW under http://dx.doi.org/10.1002/anie.201105104.

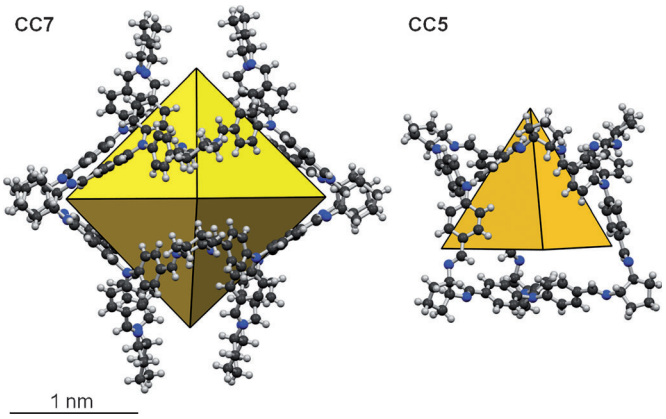


***Figure 1.*** Single-crystal X-ray structures of **CC7** and the [4+6] tetrahedral cage **CC5**[25] (1 nm scale bar). The yellow octahedron and tetrahedron are included to visualize the shape of the cavity.

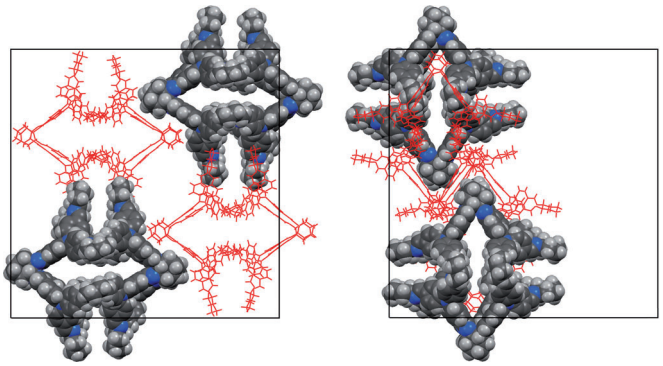

***Figure 2.*** Packing diagram for **CC7** solvate showing one half of the unit cell content: view down *c* axis (left) and *b* axis (right). Crystallographically independent molecules are distinguished by space-filling and wireframe representations. **CC8** (not shown) packs isostructurally.

into the dichloromethane and helps in stabilizing the crystal. Both cages have tetrahedral *T* symmetry, and by defining the central amine nitrogen atoms in the 8 **A** units (Scheme 1) as nodes, its topology is equivalent to that of the [8+12] chiral nanocube structure proposed by Warmuth.[23] The 8 triphenylamine moieties occupy the vertices and the 12 diamine linkers occupy the edges of this highly distorted cube (Figure S4). By contrast, the molecular shape, as opposed to the topology, has more similarities with the structural model proposed for a rhombicuboctahedral capsule.[22] That is, the 6 neighboring "pairs" of cyclohexanediamine linkers describe an octahedron with an edge length of 1.5 nm and a cavity volume of approximately 1500 $Å^3$ (Figure 1). The cage is significantly larger than our previous largest example **CC5**[25] (see comparison in Figure 1) and approximately the same size as the highly porous adamantoid cage reported by Mastalerz et al. (2.9 nm vs 2.84 nm diameter).[9]

Upon desolvation, both **CC7** and **CC8** became amorphous (Figure S5). The desolvated materials were not found to be porous to $N_2$ at 77 K, unlike other crystalline cage phases,[5–10,25] although amorphous **CC8** did adsorb small quantities of $CO_2$ (Figures S6–S8) at ambient temperatures. This suggests that the large voids in the solvated crystalline phases collapse upon solvent removal, or at least that they become disconnected in the amorphous solid.

The need for structural rigidity to promote shape persistence in molecular cages is widely recognized but perhaps not understood in detail. For example, exactly how much rigidity is required, how do flexible cages collapse, and what precisely drives this behavior in terms of thermodynamics? We therefore investigated **CC7** with a series of molecular simulations to understand how to design large cages that are shape-persistent, and thus highly porous. For a solvent-free cage structure obtained from X-ray diffraction data—that is, an "in silico desolvated"[4] structure—energy minimization calculations using an adapted force field[26,27] showed that the cages collapsed during the simulation (Figure 3) with a large isotropic compression of the cell of over 50%. At finite temperatures, the cell was found to compress even further during molecular dynamics (MD) simulations,[28] by over 58% compared to the crystal structure during a 10 ns simulation. Most of this collapse was complete within 0.1 ns. The resulting collapsed cage structure has a skeletal density of 1.058 $g\,cm^{-3}$. As shown in Figure 3b, there is no longer an interconnected

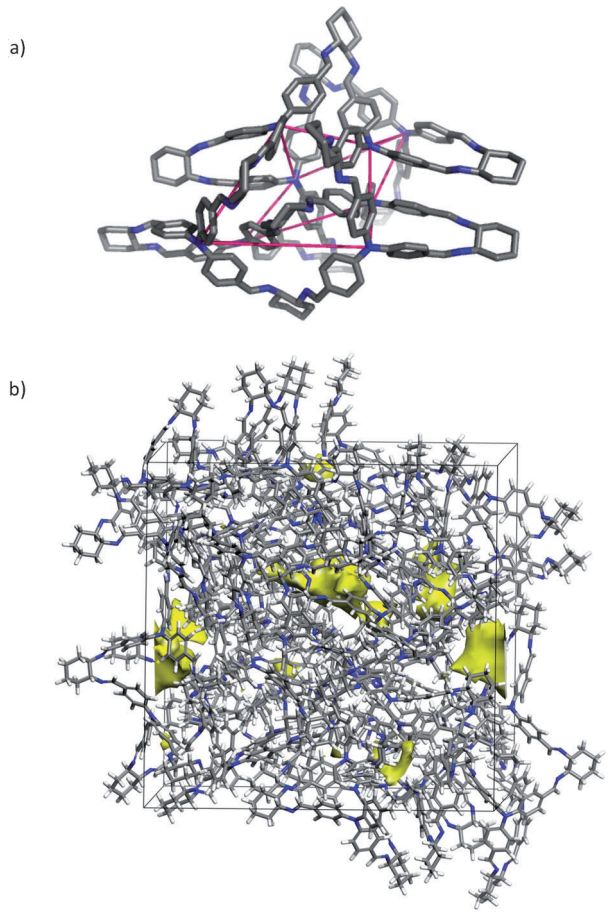


***Figure 3.*** a) A representative collapsed cage. Distortion of the original cubic topology is illustrated by the pink lines connecting the cage faces. b) Unit cell from the final configuration of a 10 ns NPT MD simulation of a desolvated **CC7** cell. The solvent-accessible surface, using a probe radius of 1.82 Å (the kinetic radius of $N_2$), is shown in yellow, demonstrating that the collapsed structure is formally nonporous to $N_2$.

  

pore network. This mechanism would explain why **CC7** becomes nonporous and amorphous upon desolvation.

To confirm that the collapse of the cage molecules was physical, and not an artifact of any inaccuracies in the force field (Figure S7), we carried out DFT-D3 calculations with the Grimme dispersion correction[29] using the PBE[30] functional and TZVP-MOLOPT basis sets[31] in the CP2K/QUICKSTEP program.[32,33] Single cages were fully geometry-optimized to compare the relative energies of the quasi-cubic topology cage from the single-crystal structure with a representative collapsed cage from the final configuration of the 10 ns MD simulation (see Figures 1 and 3a). The single collapsed cage, which contains 512 atoms, was found to be 686 kJ mol$^{-1}$ lower in energy than the "porous" cage as taken from the single-crystal structure and geometry-optimized. This large energy difference can be attributed to an increase in dispersive interactions caused by the loss of the cage void and, in particular, the formation of multiple π-π stacking interactions from arene species on opposing faces (Figure 3a). This behavior is reminiscent of structural transitions in the bistable metal–organic framework MIL-53.[34]

Interestingly, when the unit cell was loaded with 480 dichloromethane molecules and the equivalent 10 ns MD simulation was run, there was no collapse of the cage molecules. In this case, the quasi-cubic shape was maintained (Figure S8). A compression of the unit cell by 11% at the beginning of the MD run can be attributed to the 25% underloading of dichloromethane compared to the experimental (60 dichloromethane molecules per cage compared to 75–80 from crystallography). The location of the dichloromethane molecules was also monitored during the simulation; on average, 20 molecules are located inside the cage void and, hence, two thirds of the dichloromethane molecules are located in the pores between the cages. The retention of the cage shape can be attributed to the dichloromethane molecules acting as disordered space fillers inside the cage cavities, preventing their collapse.

A close inspection of the simulated collapse mechanism shows that two structural features of **CC7** might be responsible. First, there is relatively unrestricted rotation about the $C_{arene}$-$C_{arene}$-$C_{imine}$-$N_{imine}$ torsion at the cage vertex, and also the $C_{arene}$-$C_{arene}$-$N_{amine}$-$C_{arene}$ torsional angle on the tris(4-formylphenyl)amine face of the cage. This "double flexibility" allows a vertex of the cage to fold inwards, and hence to fill the cage void. Second, and as a consequence of the vertices folding inwards, the arene species on opposing faces are brought together to form π-π stacking interactions. For example, the typical intramolecular arene–arene distance decreases from 9.7 Å to 4.2 Å as a result of this collapse. There are 12 collapsible vertices on every cage, and the sequence in which they collapse appears to be random in the MD simulation. Coupled with the range of alternative packing modes that results between neighboring collapsed cages, this amorphizes the material, in agreement with the experimental results.

By contrast, MD simulations for solvent-free crystal structures of the porous cages that we reported previously (**CC2**,[6] **CC3**,[6] and **CC5**[25]) showed that both the cage shape and the interconnected porous channels were maintained during 5 ns NPT simulations (see the Supporting Information). This suggests that the force field is reliable and provides interesting clues as to why some organic cages are shape-persistent and stable to desolvation, and others are not. The smaller [4+6] cages **CC2** and **CC3** lack the additional flexibility provided by the tris(4-formylphenyl)amine units that allow for bond rotation in the plane of the face. It is therefore highly unfavorable for a vertex to fold into the cage cavity. By contrast, in the larger [4+6] cage, **CC5**,[25] the same flexible torsions observed in **CC7** are present, and **CC5** is indeed observed to be significantly more flexible in MD simulations. However, the [4+6] stoichiometry in **CC5** results in a different topology and a much smaller cage void compared to the [8+12] cage, **CC7**. Although the cavity size in **CC5** is sufficiently large to allow a vertex to fold inwards, there is no structural possibility of gaining intramolecular π-π stacking interactions between the arene faces (Figure S9).

To synthesize larger shape-persistent organic cages in the future, one might consider how to frustrate the collapse mechanism proposed herein. First, preventing rotation in the plane of the cage face would be beneficial. This was tested in MD simulations whereby the atoms involved in this rotation in the **CC7** face were fixed as rigid bodies (Figures S10 and S11). This slowed but did not prevent the compression of the cage; partial collapse occurred at a simulation temperature of 373 K. Interestingly, though, no collapse occurred at 273 K over the whole 5 ns run. One synthetic approach to rigidifying the cage faces might be to use larger fused polyaromatic hydrocarbons, since out-of-plane deformations would be highly disfavored. Cage collapse could also be inhibited by designing cages that cannot form additional favorable interactions, such as π-π stacking, upon collapse, or by "pinning" structures into a quasi-cubic topology through intramolecular noncovalent interactions, or perhaps by using post-synthetic "cross-linking" strategies.[35]

In essence, the single-crystal structures for **CC7** and **CC8** represent cages in a "sea" of solvent molecules. Hence, one might expect similar structures to persist in true molecular solutions. The $^1$H NMR spectra of **CC7** recorded at 20 °C and at 50 °C showed two distinct imine proton signals ($\delta = 8.25$ and 8.35 ppm), instead of the single imine environment observed for the smaller [4+6] cages (Figure S24).[6,13] There are also two imine carbon resonances ($\delta = 159.2$ and 159.3 ppm) in the $^{13}$C NMR spectrum. This confirms the presence of two distinct imine environments in the solution structure of the **CC7** molecule that do not exchange on the NMR timescale, consistent with the crystal structure where half of the imine protons point outwards (Figure S25) and the other half towards the interior of the cage (**3′** in Figure S25). 2D COSY and HSQC NMR spectroscopy (Figure S26) for **CC7** further confirm the various resonance assignments.

The formation of **CC7** also demonstrates the strong sensitivity of dynamic covalent assembly reactions to small changes in the substrates. For example, a [4+6] cage (**CC5**; Figure 1)[25] forms rather than the [8+12] **CC7** species when (*R*,*R*)-1,2-cyclopentanediamine is used in place of the cyclohexane analogue under otherwise similar reaction conditions. We do not have an explanation for this, though we speculate that the difference may be caused by small cumulative

  

differences in steric strain in the respective cage vertices for **CC5** and **CC7**. This observation can be compared with the sharp structural switch in large metal–organic polyhedra upon subtle ligand variation, suggesting a degree of "emergent" behavior in these multicomponent systems.[24a]

In summary, we have demonstrated the dynamic covalent synthesis of two large chiral organic cages, **CC7** and **CC8**, with inner diameters of 1.2 nm. This occurs as a one-pot self-assembly reaction involving 20 relatively simple molecules. For context, the cavities in these cages are similar in scale to a $Au_{55}$ nanocluster (Figure S28). One can also carry out chemistry on these systems: for example, **CC7** can be cleanly reduced to its amine form at room temperature using $NaBH_4$ in a mixture of $CHCl_3$ and MeOH, as supported by NMR spectroscopy and mass spectrometry (Figures S29 and S30). In terms of porous materials, the experimental data and MD simulations presented herein highlight the challenge in producing mesoporous organic cage molecules. However, the MD simulations also give insight into the probable mode of cage collapse for **CC7**, as well as suggesting strategies for avoiding this in future analogues.

## Experimental Section

Synthesis of **CC7**: Dichloromethane (200 mL) was added slowly to **A** (1.32 g, 4 mmol) in an oven-dried 500 mL round-bottom flask at room temperature. After 10 min, a solution of **B1** (689 mg, 6 mmol) in dichloromethane (200 mL) was added slowly down by the inside wall of the flask. The resulting mixture was kept at room temperature without stirring. After 48 h, a clear pale-yellow solution was observed which contained a large amount of colorless crystals with cubic morphology floating on the top of the solution. The solids were removed by filtration, washed with dichloromethane (3 × 5 mL), and afforded pure **CC7** after air-drying in 87% yield (1.55 g). Single-crystal data were obtained from a crystal grown in dichloromethane. $^1$H NMR ($CDCl_3$, 400 MHz): $\delta = 8.35$ (s, 12H), 8.25 (s, 12H), 7.61 (m, 48H), 7.07 (m, 48H), 3.52 (br m, 24H), 1.77–1.88 (br s, 72H), 1.55 ppm (br s, 24H). $^{13}$C NMR ($CDCl_3$, 100 MHz): $\delta = 159.4$, 159.3, 148.9, 148.6, 131.8, 131.6, 129.4, 124.1, 123.9, 75.1, 74.5, 33.6, 24.6 ppm. ESI-MS (MeOH/$CHCl_3$): $m/z = 1785.5$ for $C_{240}H_{240}N_{32}$ $[M+2H]^{2+}$, 1190.7 for $C_{240}H_{240}N_{32}$ $[M+3H]^{3+}$; MALDI-TOF MS: $m/z = 3573$ for $C_{240}H_{240}N_{32}$ $[M+H]^+$.

Molecular simulations: Energy minimization calculations were performed using the Forcite module of the Materials Studio 5.0 software package (Accelrys, San Diego, CA, 2009) and our in-house force field, previously adapted from PCFF[26] to describe porous organic cages.[27] Molecular dynamics simulations were run in the DL_POLY2.20 program[28] in an NPT ensemble with the Nosé–Hoover thermostat at 373 K, 1 atm and a timestep of 0.5 fs (for full simulation details see the Supporting Information).

Received: July 20, 2011
Published online: September 16, 2011

**Keywords:** flexibility · imines · molecular dynamics · porous organic cages · self-assembly

[1] M. Mastalerz, *Angew. Chem.* **2010**, *122*, 5164; *Angew. Chem. Int. Ed.* **2010**, *49*, 5042.
[2] F. Hof, S. L. Craig, C. Nuckolls, J. Rebek, Jr., *Angew. Chem.* **2002**, *114*, 1556; *Angew. Chem. Int. Ed.* **2002**, *41*, 1488.
[3] A. V. Leontiev, D. M. Rudkevich, *Chem. Commun.* **2004**, 1468.
[4] L. J. Barbour, *Chem. Commun.* **2006**, 1163.
[5] T. Tozawa et al., *Nat. Mater.* **2009**, *8*, 973.
[6] N. B. McKeown, *J. Mater. Chem.* **2010**, *20*, 10588.
[7] J. R. Holst, A. Trewin, A. I. Cooper, *Nat. Chem.* **2010**, *2*, 915.
[8] M. Mastalerz, *Chem. Commun.* **2008**, 4756.
[9] M. Mastalerz, M. W. Schneider, I. M. Oppel, O. Presly, *Angew. Chem.* **2011**, *123*, 1078; *Angew. Chem. Int. Ed.* **2011**, *50*, 1046.
[10] A. Granzhan, T. Riis-Johannessen, R. Scopelliti, K. Severin, *Angew. Chem.* **2010**, *122*, 5647; *Angew. Chem. Int. Ed.* **2010**, *49*, 5515.
[11] T. Hasell, X. Wu, J. T. A. Jones, J. Bacsa, A. Steiner, T. Mitra, A. Trewin, D. J. Adams, A. I. Cooper, *Nat. Chem.* **2010**, *2*, 750.
[12] J. Chen, S. Korner, S. L. Craig, D. M. Rudkevich, J. Rebek, Jr., *Nature* **2002**, *415*, 385.
[13] P. Skowronek, J. Gawronski, *Org. Lett.* **2008**, *10*, 4755.
[14] M. J. MacLachlan, *Pure Appl. Chem.* **2006**, *78*, 873.
[15] N. E. Borisova, M. D. Reshetova, Y. A. Ustynyuk, *Chem. Rev.* **2007**, *107*, 46.
[16] S. J. Rowan, S. J. Cantrill, G. R. L. Cousins, J. K. M. Sanders, J. F. Stoddart, *Angew. Chem.* **2002**, *114*, 938; *Angew. Chem. Int. Ed.* **2002**, *41*, 898.
[17] P. R. Ashton, N. S. Isaacs, F. H. Kohnke, G. S. Dalcontres, J. F. Stoddart, *Angew. Chem.* **1989**, *101*, 1269; *Angew. Chem. Int. Ed. Engl.* **1989**, *28*, 1261.
[18] H. M. El-Kaderi, J. R. Hunt, J. L. Mendoza-Cortes, A. P. Côté, R. E. Taylor, M. O'Keeffe, O. M. Yaghi, *Science* **2007**, *316*, 268.
[19] M. L. C. Quan, D. J. Cram, *J. Am. Chem. Soc.* **1991**, *113*, 2754.
[20] X. Liu, Y. Liu, G. Li, R. Warmuth, *Angew. Chem.* **2006**, *118*, 915; *Angew. Chem. Int. Ed.* **2006**, *45*, 901.
[21] X. Liu, R. Warmuth, *J. Am. Chem. Soc.* **2006**, *128*, 14120.
[22] Y. Liu, X. Liu, R. Warmuth, *Chem. Eur. J.* **2007**, *13*, 8953.
[23] D. Xu, R. Warmuth, *J. Am. Chem. Soc.* **2008**, *130*, 7520.
[24] a) Q. F. Sun, J. Iwasa, D. Ogawa, Y. Ishido, S. Sato, T. Ozeki, Y. Sei, K. Yamaguchi, M. Fujita, *Science* **2010**, *328*, 1144; b) S. R. Seidel, P. J. Stang, *Acc. Chem. Res.* **2002**, *35*, 972.
[25] J. T. A. Jones, T. Hasell, X. F. Wu, J. Bacsa, K. E. Jelfs, M. Schmidtmann, S. Y. Chong, D. J. Adams, A. Trewin, F. Schiffmann, F. Cora, B. Slater, A. Steiner, G. M. Day, A. I. Cooper, *Nature* **2011**, *474*, 367.
[26] H. Sun, *Macromolecules* **1995**, *28*, 701.
[27] J. T. A. Jones, D. Holden, T. Mitra, T. Hasell, D. J. Adams, K. E. Jelfs, A. Trewin, D. J. Willock, G. M. Day, J. Bacsa, A. Steiner, A. I. Cooper, *Angew. Chem.* **2011**, *123*, 775; *Angew. Chem. Int. Ed.* **2011**, *50*, 749.
[28] W. Smith, C. W. Yong, P. M. Rodger, *Mol. Simul.* **2002**, *28*, 385.
[29] S. Grimme, J. Antony, S. Ehrlich, H. Krieg, *J. Chem. Phys.* **2010**, *132*, 154104.
[30] J. Perdew, K. Burke, M. Ernzerhof, *Phys. Rev. Lett.* **1996**, *77*, 3865.
[31] J. Vandevondele, J. Hutter, *J. Chem. Phys.* **2007**, *127*, 114105.
[32] J. Vandevondele, M. Krack, F. Mohamed, M. Parrinello, T. Chassaing, J. Hutter, *Comput. Phys. Commun.* **2005**, *167*, 103.
[33] The CP2K development group; http://cp2k.berlios.de/.
[34] A. M. Walker, B. Civalleri, B. Slater, C. Mellot-Draznieks, F. Cora, C. M. Zicovich-Wilson, G. Roman-Perez, J. M. Soler, J. D. Gale, *Angew. Chem.* **2010**, *122*, 7663; *Angew. Chem. Int. Ed.* **2010**, *49*, 7501.
[35] C. G. Bezzu, M. Helliwell, J. E. Warren, D. R. Allan, N. B. McKeown, *Science* **2010**, *327*, 1627.

  